Supporting Material

Incorporation of Substitutionally Labile $[V^{III}(CN)_6]^{3-}$ into Prussian Blue-Type Magnetic Materials

Kendric J. Nelson and Joel S. Miller

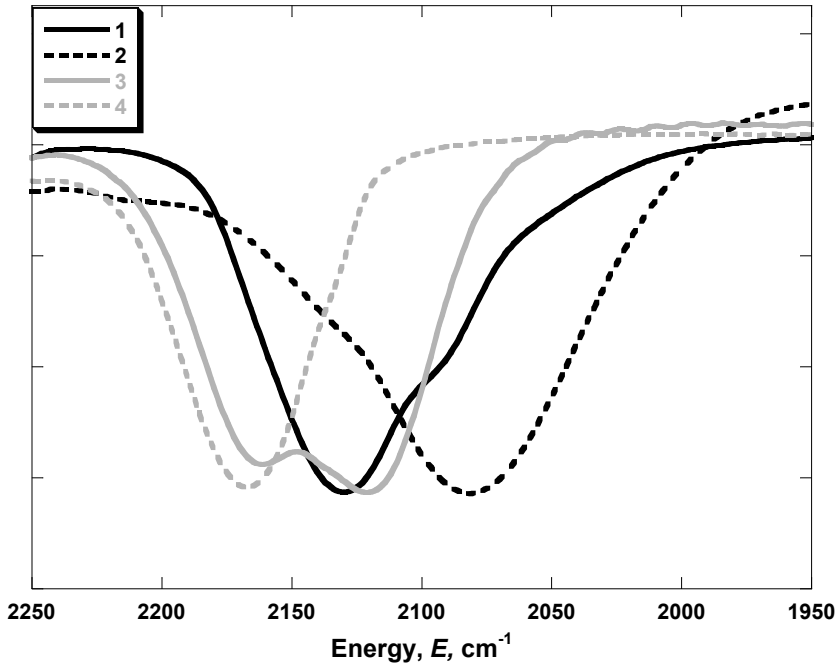

Figure S1. ν_{CN} region of $Mn_{1.5}[V(CN)_6]$•0.30(MeCN) (**1**), $Fe_{0.5}V[Fe(CN)_6]$•0.85(MeCN) (**2**), $(NEt_4)_{0.10}Co_{1.5-a}V_a[Co(CN)_6]_a[V(CN)_6]_{1-a}(BF_4)_{0.10}$•0.35(MeCN) (**3**), and $(NEt_4)_{0.20}V[Ni(CN)_4]_{1.6}$•0.10-(MeCN) (**4**).

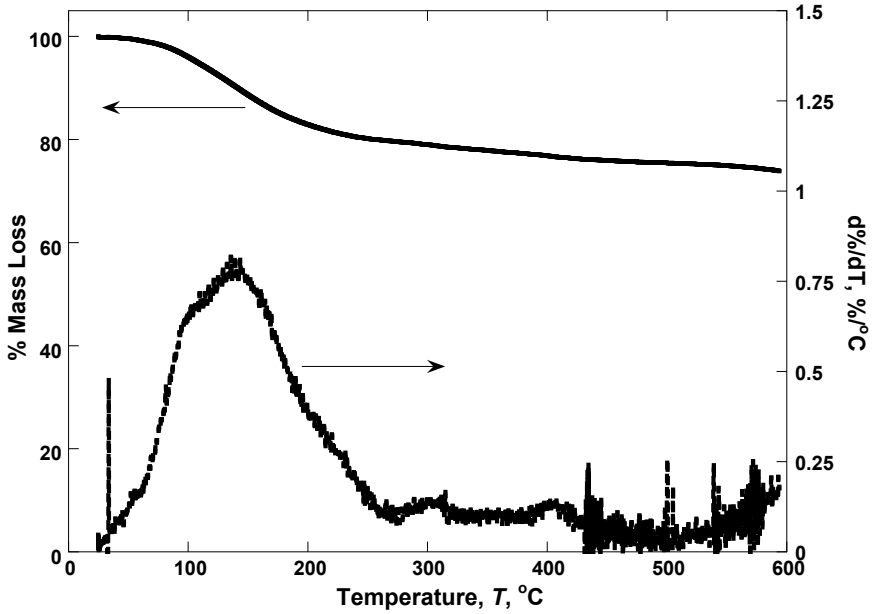

Figure S2. TGA trace of $Mn_{1.5}[V(CN)_6]$•0.30(MeCN), **1**, at a heating rate of 10 °C/min.

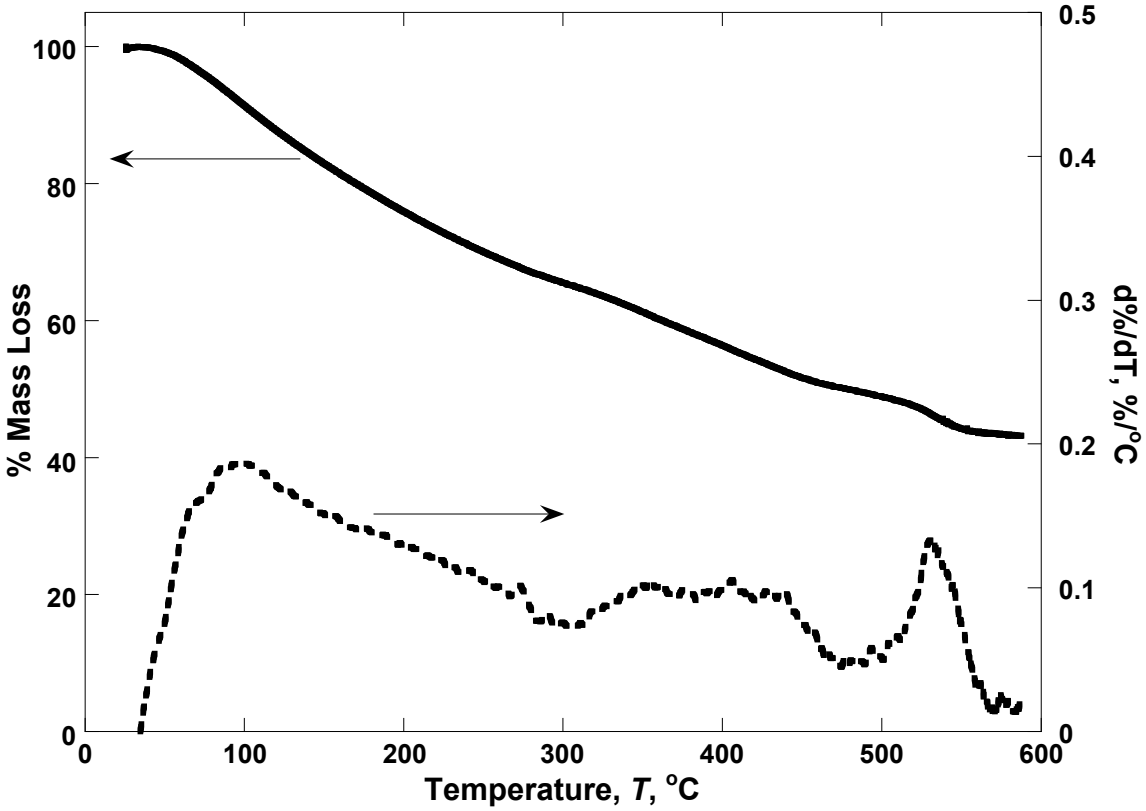

Figure S3. TGA trace of $Fe_{0.5}V[Fe(CN)_6]$•0.85(MeCN), **2**, at a heating rate of 10 °C/min.

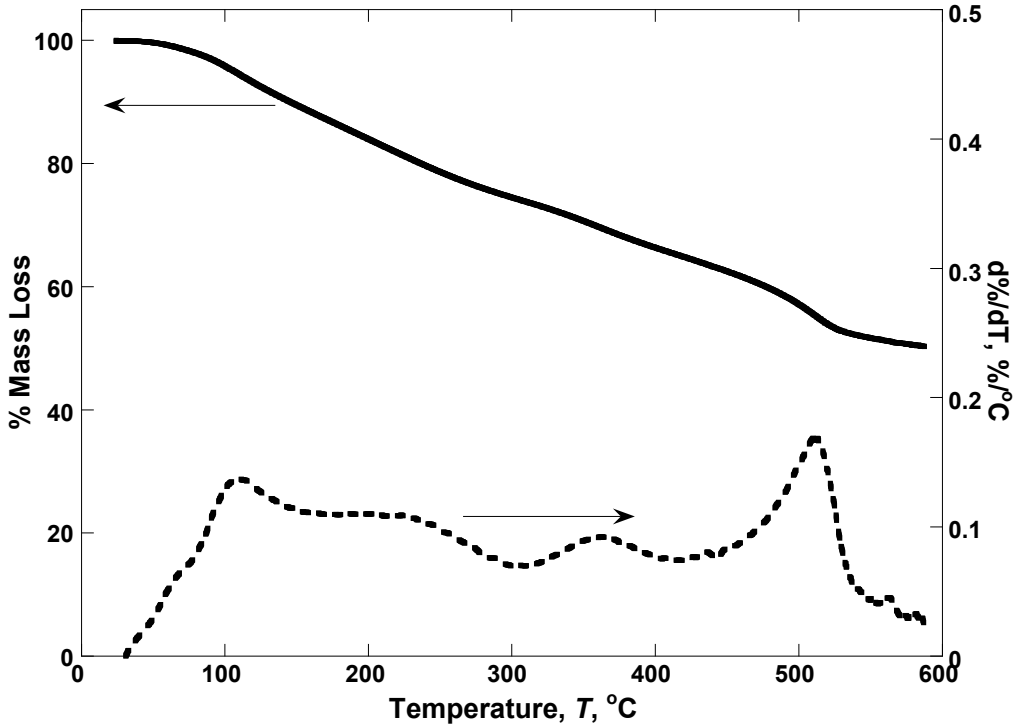

Figure S4. TGA trace of $(NEt_4)_{0.10}Co_{1.5-a}V_a[Co(CN)_6]_a[V(CN)_6]_{1-a}(BF_4)_{0.10}$•0.35(MeCN), **3**, at a heating rate of 10 °C/min.

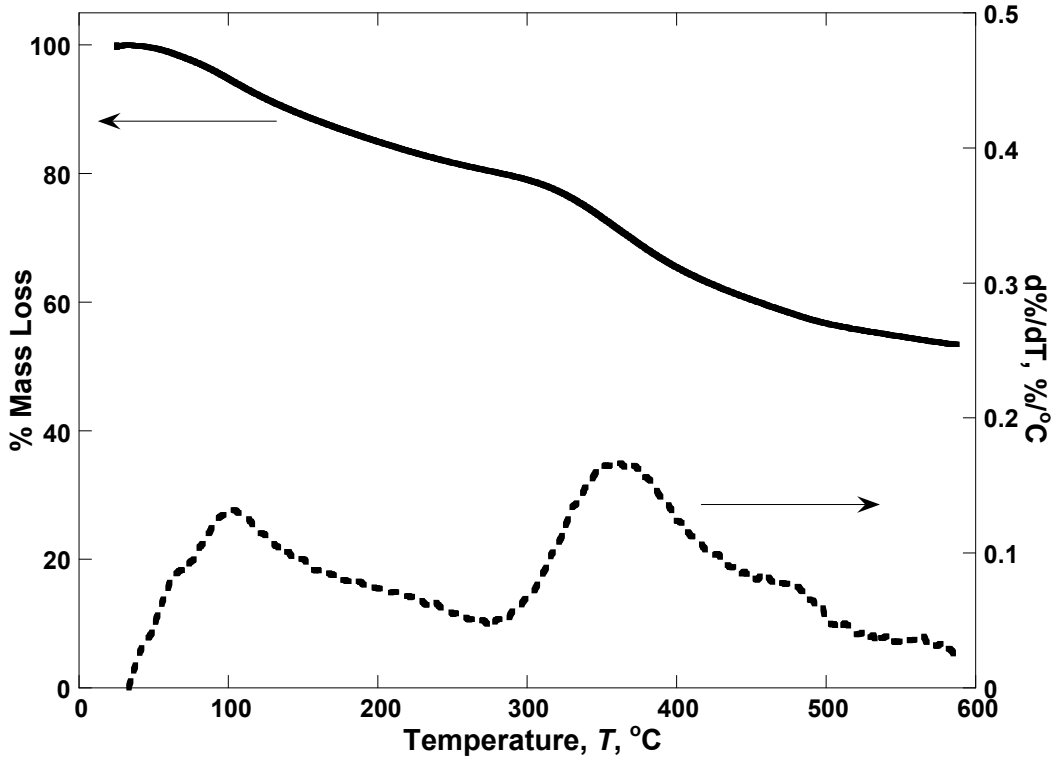

Figure S5. TGA trace of $(NEt_4)_{0.20}V[Ni(CN)_4]_{1.6}$•0.10(MeCN), **4**, at a heating rate of 10 °C/min.

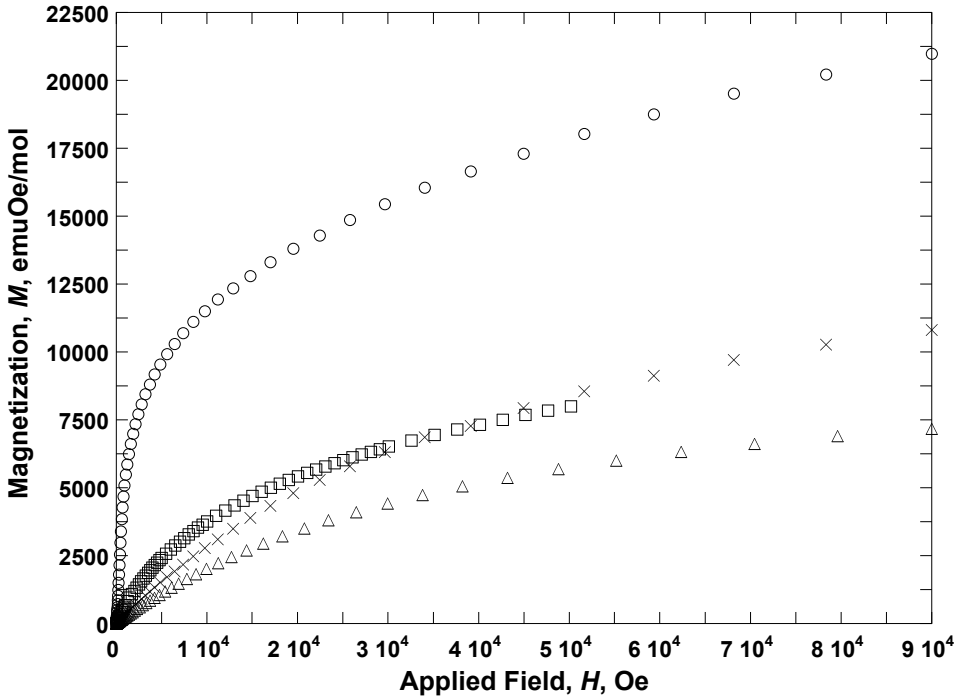

Figure S6. *M*(*H*) data for $Mn^{II}_{1.5}[V^{III}(CN)_6]$•0.30(MeCN), **1** (o), $Fe^{II}_{0.5}V^{III}[Fe^{II}(CN)_6]$•0.85(MeCN), **2** (□), $(NEt_4)_{0.10}Co^{II}_{1.5-a}V^{II}_a[Co^{III}(CN)_6]_a[V^{III}(CN)_6]_{1-a}(BF_4)_{0.10}$•0.35(MeCN), **3** (x), and $(NEt_4)_{0.20}V$-$[Ni(CN)_4]_{1.6}$•0.10(MeCN), **4** (Δ).